



ELSEVIER

Contents lists available at SciVerse ScienceDirect

Talanta

journal homepage: www.elsevier.com/locate/talanta

Ability of various materials to detect explosive vapors by fluorescent technologies: A comparative study[☆]

Myriam Bouhadid^a, Thomas Caron^{a,b}, Florian Veignal^a, Eric Pasquinet^a, Amédée Ratsimihety^b, François Ganachaud^b, Pierre Montméat^{a,*}

^aCEA-DAM Le Ripault, BP 16, F-37260 MONTS, France

^bEcole de Chimie, rue de l'Ecole Normale, F-34000 Montpellier, France

ARTICLE INFO

Article history:

Received 30 January 2012

Received in revised form

12 June 2012

Accepted 15 June 2012

Available online 14 July 2012

Keywords:

Detection

Explosives

Fluorescent material

Chemical sensors

ABSTRACT

For the development of fluorescent sensors, one of the key points is choosing the sensitive material. In this article, we aim at evaluating, under strictly identical experimental conditions, the performance of three materials for the detection of dinitrotoluene (a volatile marker of trinitrotoluene) through different parameters: response time, fluorescence intensity, sensitivity, reversibility, reaction after successive exposures and long-term stability. The results are discussed according to the nature of the sensitive materials. This first study rendered it possible to select a conjugated molecule as the best sensitive material for the development of a lab-made prototype. In a second part, the selectivity of this particular sensitive material was studied and its ability to detect TNT could be demonstrated.

© 2012 Published by Elsevier B.V.

1. Introduction

The increased use of explosives in terrorist activities has created a demand for a continued innovation in the detection of these agents. To this aim, the detection of nitroaromatic compounds (NAC) using chemical sensors has been the major goal of our team for almost a decade. Fluorescent sensors especially seem to satisfy requirements in terms of reliability, cost and handling ability. In this field, an optical device based on the capability of various materials to detect explosive vapors, particularly nitroaromatic compounds such as trinitrotoluene TNT and dinitrotoluene DNT, has been developed [1]. TNT is one of the most commonly used explosives for military applications and DNT is a significant part in the chemical signature of this target compound [2].

The design of a sensor requires several steps. One of the key points is the choice of the sensitive material. According to the literature, various materials [3–17] have been used for the detection of nitroaromatic compounds (NACs) but very few comparisons of data between different families have been published. Our work has focused on the comparison of the responses of three distinctly different organic compounds for the fluorescence detection of

nitroaromatic explosives, i.e. a π -conjugated phenylene-ethynylene diimine, a conjugated polymer (polypentiptycene) and a polycarbosi-lane functionalized with fluorescent pyrene groups. The first two sensitive layers have been reported to detect nitroaromatic explosives even at low concentrations [4,17–19]. Fluorescent polycarbosi-lane has also been described as an efficient sensitive material [12]. Indeed, their viscoelastic properties and high gas permeability make these silicium-based polymers, among which are silicones, interesting candidates for chemical sensors [10,11,13,20].

The objective of this study was to first evaluate, under strictly identical conditions, some performance parameters of the three materials with regard to the detection of DNT (as a volatile marker of TNT) [2]: response time, fluorescence intensity, sensitivity, reversibility, and reaction after successive exposures. The results are discussed according to the nature of the sensitive materials. The effect of interfering compounds (acetone, ethanol, hydrogen peroxide, etc.) and the detection of explosive vapors (e.g., TNT) with the sensitive material exhibiting the best global detection performances is also presented.

2. Experimental part

2.1. Materials

The selected materials included a π -conjugated phenylene-ethynylene diimine (material 1), polypentiptycene (material 2) and a fluorescent polycarbosi-lane (material 3) whose chemical

[☆]Memory—These authors want to dedicate this paper to Etienne Kosciusko-Morizet, we hope that it will contribute to help keep the memory of him alive.

* Corresponding author. Tel.: +33 2 47 34 56 79; fax: +33 2 47 34 51 58.

E-mail address: pierre.montmeat@cea.fr (P. Montméat).

Table 1
Three fluorescent materials studied in this work and their main characteristics.

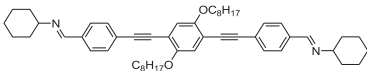
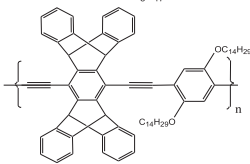
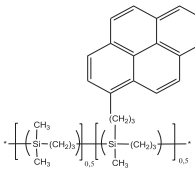
Sensitive material	Chemical structure	Nature	Main characteristics
Material 1: π -conjugated phenylene–ethylene diimine		Molecule/Oligomer	Non-Porous, π -conjugated
Material 2: polypentiptycene		Solid polymer	Porous, π -conjugated, fluorescent quenching amplification effect
Material 3: fluorescent polycarbosilane		Viscous liquid polymer	Viscoelastic properties, high gas permeability

Table 2
Listing and characteristics of analytes used in this study.

Analyte	Nature	P_{vap} at 25 °C
MEK	Interfering	100,000 ppmv
Acetone	Interfering	240,000 ppmv
EtOH	Interfering	58,000 ppmv
CHCl ₃	Interfering	210,000 ppmv
H ₂ O ₂ 30 wt%	Interfering/precursor	1900 ppmv
4-NT	Taggant	80 ppmv
DNT	Taggant	150 ppbv
TNT	Explosive	5 ppbv
DMNB	Taggant	2700 ppbv*

structures and main properties are given in Table 1. The synthesis of each material has been previously reported by our group for materials 1 [5] and 3 [12] and by Yang and Swager [17] for material 2. The three syntheses were carried out in our laboratory. The molecular structures of sensitive materials 1 and 2 are closely related, as they are both conjugated phenylene–ethynylene compounds with long alkoxy lateral chains. However, they differ significantly with regard to macroscopic properties: polymer 2 exhibits a certain degree of porosity due to the bulky iptycene moieties, while compound 1 is essentially non-porous. The specific surfaces were measured by BET analysis and were found to be 3 and 36 m² g⁻¹, respectively, for material 1 and material 2. The emission fluorescence spectra of the corresponding thin films were recorded using a Fluoromax 3 spectrofluorometer (Jobin Yvon), at ambient temperature, and at an excitation wavelength of $\lambda_{ex} = 370$ nm.

In our study, the sensors were exposed to various compounds which were common interfering compounds, markers or explosives. With the exception of TNT, which was fabricated in the laboratory, all chemicals were purchased from Aldrich Chemical Co., Inc. and used as received: 2-butanone (MEK), 78-93-3; acetone, 67-64-1; ethanol (EtOH), 64-17-5; chloroform, 67-66-3; hydrogen peroxide 30% wt (H₂O₂), 7722-84-1; 2,4-dinitrotoluene (DNT), 121-14-2; 4-nitrotoluene (4-NT), 99-99-0; 2,3-dimethyl-2,3-dinitrobutane (DMNB), 3964-18-9.

Caution: TNT is highly explosive and must be handled with care.

Table 2 presents the vapor pressures (P_{vap}) of these compounds at 20 °C. H₂O₂ was chosen as a representative precursor of various peroxide explosives. DMNB and 4-NT were used as taggants in some commercial explosive compositions. DNT is a relevant marker for TNT.

3. Methods

3.1. Fluorescent prototype

The prototype used for the detection by fluorescence has been described in detail elsewhere [4]. The central element was a conventional microscope slide (75 mm × 25 mm × 1 mm) acting both as a transducer and the substrate of the active material. A typical device was composed of four sensing areas of 1.4 mm², and each of these sensing areas was successively orthogonally excited using focused LED emission. Finally, the detection of the corresponding fluorescence emission was synchronized.

The excitation module was composed of four low-cost light emitting diodes (NSHU550A, NICHIA Corporation) delivering an optical power of 0.6 mW at a wavelength of 378 nm. Light was focused on the sensor areas through two ball lenses (uncoated, 5 mm diameter, LaSFN9, Melles Griot) with a spot diameter of 1.47 mm (full-width at half maximum). A single band pass filter (330WB80, Omega Optical) was incorporated between the two series of lenses to reject wavelengths below 250 nm and above 400 nm. The illumination time was 22 ms, and the delay between two acquisitions was 60 s.

Fluorescence was guided in the slide by total internal reflection and was directly collected at the end-face by a photomultiplier tube (H8249-101, Hamamatsu). The detector was interfaced with a bandpass filter (400ALP/E, Omega Optical) and a high-pass colored filter (OG570, Schott) to suppress the remaining excitation radiation. The emission wavelengths collected by this prototype were greater than 420 nm. The elevated collection efficiency of the transducer rendered the use of imaging optics unnecessary, thus increasing the robustness, compactness, and simplicity of the system. The transducer was embedded into a home-made fluidic reaction chamber fabricated in aluminum and coated with black PTFE. The flow channel was 6 mm in width, 0.130 mm in height, and 46 mm in length. The fluidic circuitry was composed of 1/8" PTFE tubes, and the whole prototype was 40 cm × 30 cm × 16 cm.

The system was controlled with a single-board computer (BL2120 Smartcat, Z-World, USA) that had been programmed using Dynamic C[®] language. This board had a LCD/Keypad window where the measurements were displayed. Another computer was also interfaced using an RS232 serial bus, and Microsoft[®] Office Excel macros were written to interact with the single-board computer. The developed software was able to display real-time graphics and to select experimental parameters

such as PMT settings as well as the measurement frequency. The noise was near 2.5% and the signal of detection is generally supposed to be significant when it is larger than three times the noise. Here, that is to say, the signal was greater than 7.5%.

For the fluorescence measurements, each material was deposited on the entire surface of a glass substrate (microscope slides, 75 mm × 25 mm × 1 mm) by spin-coating (Braive Instrument's spin-coater at 600 rpm) from a chloroform solution during 60 s of drying. The concentrations of the solutions were 1.5 mg/mL for material 1, 5 mg/mL for material 2 and 2.3 mg/mL for material 3. These concentrations were determined in order for the fluorescence signal to be contained by 3 and 10 V in the prototype.

3.2. Quartz crystal microbalance (QCM) prototype

The piezoelectric crystals used were 9-MHz AT-cut quartz crystals (polished surface) with gold-plated metal electrodes on both sides (AMETEK, model QA-A9M-AU M). Two faces of the 9-MHz quartz microbalance were coated with the sensitive material using the same solutions as for the glass substrate. A spray-coating instrument (Dosage 2000–FRANCE) was used to coat the QCM substrate (one pulse on both faces).

In order to satisfy the Barkausen criterion, the quartz crystal resonator was inserted in an electronic oscillator loop [21]. This electronic feedback was a typical Colpitts oscillator based on a transistor made of a common emitter. The oscillator frequency for the measurements was achieved by a frequency counter with an accuracy of ± 1 Hz. For the piezoelectric quartz used herein, the

Sauerbrey equation [22] was defined according to

$$\Delta m = -0.44 \times 10^6 A \frac{\Delta F}{F_0^2} \quad (1)$$

where Δm is the adsorbed mass in g; ΔF is the frequency shift in Hz; F_0 is the fundamental frequency of the quartz: 9×10^6 Hz; and A is the total sensitive surface of the electrodes: 0.39 cm^2 . The constant 0.44×10^6 has units of g Hz cm^{-2} .

3.3. Description of sensors tests and performance evaluation

The three materials were evaluated for the detection of vapors under dry synthetic air and real ambient air. During a typical experiment, the material was exposed to air (synthetic or ambient), organic vapors diluted in air (synthetic or ambient) for 10 min and then to air again (synthetic or ambient).

For the tests in dry air, the air (Air Liquide Synthetic Air, Alphagaz Air 1) passed through a generation cell containing 1 g of analyte with a flow rate of 20 L/h. By means of mass flow controllers (Bronkhorst EL-FLOW mass flow controller and E7100 Flow bus) and valves, the generated vapor was distributed to the prototype. The temperature of the generation cell was controlled to generate various concentrations of analyte. The generated analyte vapors were calibrated by first passing through a bubbler containing specific solvent. This was followed by HPLC analysis. Table 3 presents the various concentrations in DNT obtained by this method.

In the case of tests under ambient air, peristaltic pumps were used to generate the air flows at 20 L/h. The rate of humidity was close to 40% ($\pm 10\%$) and the temperature was 20°C ($\pm 2^\circ\text{C}$), as determined by means of a probe TESTOSTOR 171-2. The concentrations of the analytes were close to their vapor pressures.

Several parameters have been defined in order to quantify the sensor performances. All these parameters are detailed as follows:

- (1) I_0 was the fluorescence intensity before exposure.
- (2) I_{40} was the fluorescence intensity after 10 min of exposure.
- (3) I_{60} was the fluorescence intensity after 10 min of exposure followed by 20 min under air.
- (4) The response was calculated by

$$R (\%) = \left(\frac{I_0 - I_{40}}{I_0} \right) \times 100 \quad (2)$$

Table 3

Concentration of DNT as a function of the temperature of the generation cell.

Temperature of generation cell ($^\circ\text{C}$)	[DNT] (ppbv)
25	150
20	90
15	30
10	25
5	20
0	10

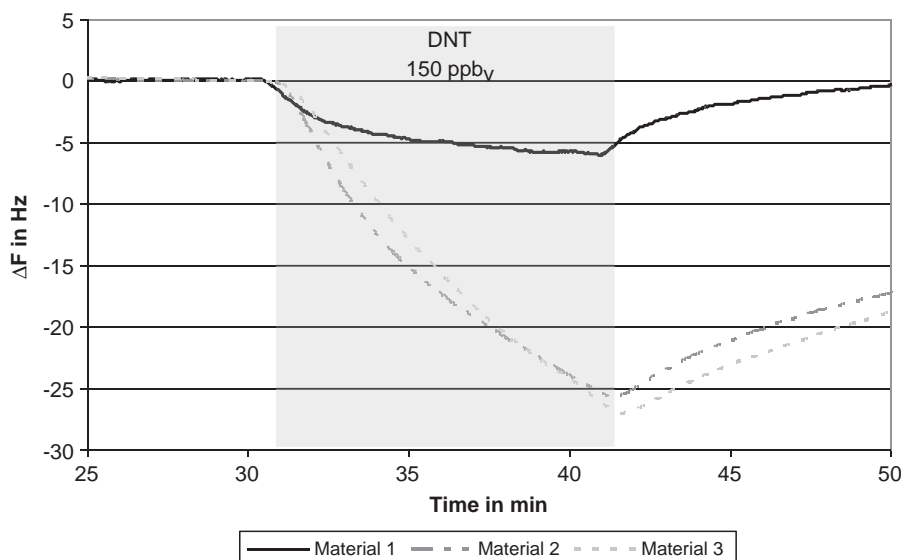


Fig. 1. Frequency of the QCM based on materials 1, 2 and 3 with a 10-min DNT exposure.

The reversibility was calculated according to:

$$R_v (\%) = \left(1 - \frac{I_0 - I_{60}}{I_0}\right) \times 100 \quad (3)$$

The sensitivity was calculated as

$$S = \frac{R}{[DNT]} \quad (4)$$

The response time (t_r) corresponded to the time sufficient to reach a significant signal, that is to say a response superior to 7.5% [4]. This time also depended on the acquisition rate, and t_r was thus determined by steps of 1 min.

4. Results and discussion

4.1. Preliminary studies via QCM analyses

In the first approach, all materials were tested with quartz crystal microbalance (QCM) technologies. These tests were performed prior to the fluorescence study to evaluate the affinity between the

different materials and DNT. Fig. 1 shows the results obtained for all materials during a 10-min exposure to ca. 150 ppb_v DNT in dry air.

For materials 2 and 3, the quartz frequency decreased substantially during DNT exposure without reaching a plateau, then increased very slowly when DNT exposure was stopped. Conversely, for material 1, the signal tended towards a plateau at a frequency shift of only 6 Hz, which is a very small value compared to other materials that have been tested under similar conditions [23]. The initial signal was recovered after only 10 min under pure air, suggesting that DNT essentially interacts physically with the surface of material 1. The far better physico-chemical affinity seen for materials 2 and 3 towards the nitroaromatic species could be linked to chemical interactions and/or to physical phenomena. Since the molecular structures of materials 1 and 2 exhibit similarities, the observed QCM behavior is believed to be related to physical phenomena rather than to chemical interactions, such as $\pi-\pi$ interactions with DNT [24]. Solubilization properties of the viscoelastic polymer 3 gave rise to a DNT adsorption pattern similar to the one observed with the more crystalline, but porous, polymer 2. Note that for these last two materials, the signals took a longer time to reach back to the baseline (not shown).

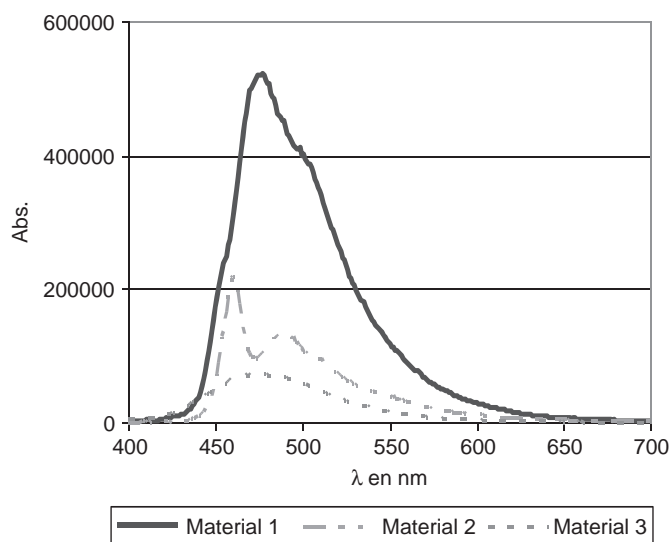


Fig. 2. Fluorescence emission intensity as a function of the material— $\lambda_{ex}=370$ nm.

4.2. Fluorescence study using a lab-made prototype

Prior to the performance analysis, emission fluorescence spectra of the thin films were obtained for all materials to insure that the fluorescence characteristics were compatible with the prototype (see experimental part). The fluorescence intensities of the three materials deposited on the glass substrate are presented in Fig. 2. When the material was excited at 370 nm (< 400 nm), the emission profile showed a maximum absorbance of $\lambda_{em} > 420$ nm, and thus was compatible with the lab-made prototype. A comparison between the three materials revealed that the fluorescence of material 1 was significantly higher than those obtained for the other two compounds.

To demonstrate the feasibility of the fluorescent sensor based on the three materials, each material was tested in our prototype based on the fluorescence technology in the presence of DNT (30 ppb_v). The obtained detection signals are shown in Fig. 3. Just as the results in QCM tests, materials 2 and 3 presented similar responses in the presence of DNT. The fluorescence decreased quickly during exposure and the reversibility was poor. For material 1, the response was weaker than for materials 2 and 3, but the reversibility was better.

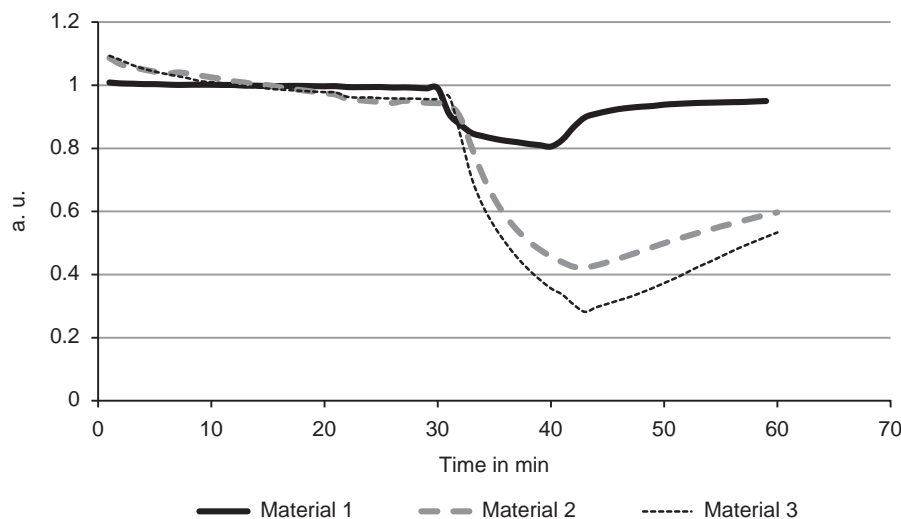


Fig. 3. Example of signal detection by fluorescence upon exposure to 30 ppb_v of DNT for 10 min.

4.3. Performances of the lab-made prototype

The performances of the sensors in terms of response time, sensitivity and reversibility were then evaluated at various concentrations of DNT in dry air.

The response time was determined for each sensitive material at various concentrations in DNT. All results are summarized in Table 4. The response time increased with decreasing DNT concentrations. This was expected since it reflected the number of fluorophores quenched, which was obviously linked to the quantity of DNT adsorbed on the surface and within the films. It is also known that the rate of DNT adsorption on the sensitive material is strongly related to the concentration of DNT in the vapor phase [25] Table 5.

Table 4
Response time of different materials as a function of concentrations of DNT.

[DNT]	Time of response (min)		
	Material 1	Material 2	Material 3
150	< 1	< 1	< 1
90	< 1	< 1	< 1
30	< 1	< 1	< 1
25	< 1–1	2	< 1
20	1–2	3–4	1–2
10	$R < 7.5\%$	3–4	2–3

Table 5
Summary of sensor performances.

[DNT] (ppbv)	Material 1			Material 2			Material 3		
	Response (%) R	Sensitivity (%/ppbv) S	Reversibility (%) R_v	Response (%) R	Sensitivity (%/ppbv) S	Reversibility (%) R_v	Response (%) R	Sensitivity (%/ppbv) S	Reversibility (%) R_v
150	28	0.2	91	78	0.5	41	76	0.5	44
90	27	0.3	93	67	0.7	37	75	0.8	46
30	18	0.6	96	49	1.6	65	62	2.1	57
25	15	0.6	95	46	1.8	56	51	2.0	74
10	6	0.6	98	17	1.7	87	20	2.0	85
Ld ^a	12 ppbv			4 ppbv			4 ppbv		

^a Ld represents the threshold for a signal/noise ratio of 3

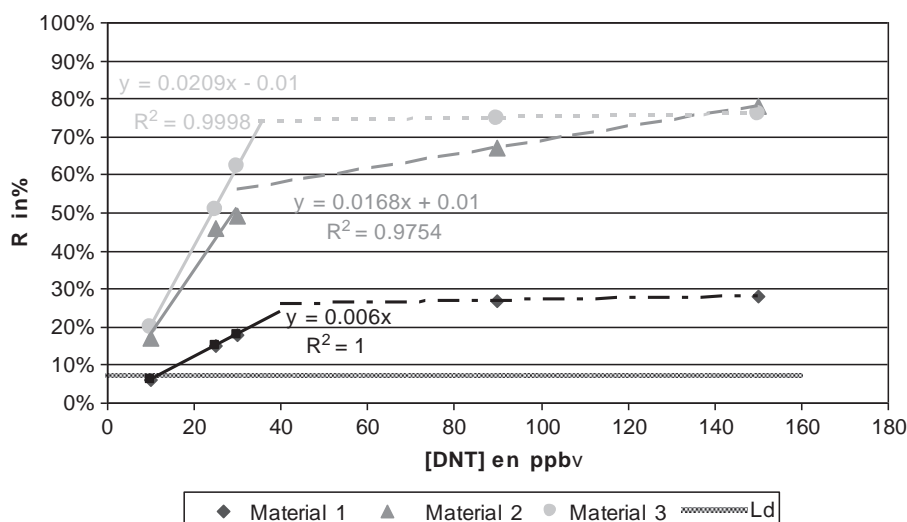


Fig. 4. Calibration curve of the sensors based on materials 1, 2 and 3.

Significantly different response times were recorded exclusively at very low concentrations. Interestingly, the response time of material 2 was slightly higher than that of materials 1 and 3, although the former polymer was supposed to exhibit an amplification effect (i.e., one DNT molecule can quench more than one fluorophore due to extensive electronic conjugation) [19]. In this particular case, this advantage may be counterbalanced by a slow diffusion within the films due to the presence of cavities and/or strong chemical π - π interactions.

The response, the sensitivity and the reversibility of the sensors are shown in Table 4. For each material, the response depended on the concentration of DNT: when the concentration of DNT increased, so did the response. The fluorescence inhibition was contained by 28 and 6% for material 1, by 78 and 17% for material 2 and by 85 and 44% for material 3. Generally speaking, the responses were sufficient for the detection of DNT.

The calibration curves for the three materials are represented in Fig. 4. These curves present two trends. The first linear slope is related to the responses of the sensors when the concentrations of DNT were smaller than 30 ppbv. The best correlation between the inhibition of fluorescence and the concentration was obtained by material 1, although, at the same concentration of exposure in DNT, the response was more significant for materials 2 and 3 as opposed to material 1. When the concentrations of DNT were greater than 90 ppbv, high responses were obtained and the curves reached a plateau, particularly in the case of materials 1 and 3.

If one considers the sensitivity obtained for low concentrations of DNT, as well as the noise level of the system (2.5%), the

detection threshold for a signal/noise ratio of 3 could be estimated to 12 ppb_v for material 1, and to 4 ppb_v for materials 2 and 3. Even if the sensitivity of material 1 was clearly lower than those of materials 2 and 3, the latter still remained very useful and might appear intriguing in view of the poor adsorption properties of material 1 (see the QCM study). The specific behavior of material 1 will be discussed in a forthcoming paper. The goal of this paper will be to study the phenomena involved during detection using fluorescence and structural properties of material 1.

The reversibility of sensors based on materials 2 and 3 was seen to decrease when the concentration of DNT increased. A satisfactory value was found when the concentration of DNT was 10 ppb_v, while it was insufficient for higher concentrations (e.g. R_v close to 40% when the concentration of DNT was 150 ppb_v). On the other hand, the reversibility of material 1 was excellent whatever the concentration of DNT. The percentage of reversibility, 20 min after exposure, was always higher than 90%. To confirm this advantage, five detection cycles were successfully recorded, corresponding to 10 min of exposure at 25 ppb_v of DNT followed by 20 min under pure air. Fig. 5 shows the fluorescence intensity of the three materials, given by the fluorescence intensity as a function of time. Again, material 1 presents the best results, with fast reversibility from the first exposure.

When it comes to the development of reliable chemical detectors, the stability of the response of the sensor is a major topic of investigation. As shown in Ref. [26], the implementation of an alarm requires a reliable data treatment thanks to a limited number of experiments. The various algorithm parameters (response time, thresholds, etc.) obtained from the few tests should support a robust sensor signal to assure their reliability. Thanks to excellent stability of signal from material 1, it was considered well adapted for the implementation of an alarm on a portable detector. Obviously, this advantageous behavior upon successive exposures was closely linked to the fact that only surface interactions took place between DNT and the non-porous material 1. Material 3 showed a medium reversibility at the first exposure, after which it became more satisfactory. Interestingly, material 3 presented better cycling properties than material 2 even though they exhibited similar adsorption schemes (see the QCM study). This suggests that the dissolution of DNT within a film of material 3 is much more reversible than adsorption

within a porous film of material 2. Obviously, viscoelastic properties and a high gas permeability account for these results, which are in agreement with the ones obtained concerning the response time.

4.4. Material choice

To summarize this part, a ranking of the materials was established and is presented in Table 6. Material 2 was very sensitive but the intensity of fluorescence as well as the reversibility was poor. Material 3 was also very sensitive, but the response time as well as the reversibility was far from optimal. Material 1 enabled a safe and reproducible detection since this material exhibited the best reversibility. Its only drawback concerned the weaker sensitivity compared to materials 2 and 3. Nevertheless, the limit of detection was estimated at ca. 12 ppb_v, which was sufficient for our application. The excellent reversibility led to a long-term stability of the sensor and thus reduced the maintenance cost of the detector. For this reason, material 1 was selected for further investigations.

4.5. Further studies with material 1

Selectivity and insensitivity to common interferents are other major considerations when developing an explosive sensor. Material 1 was exposed to different non-explosive interfering

Table 6
Ranking of materials according to their performances.

Performance	Ranking		
	Material 1	Material 2	Material 3
Intensity of fluorescence	+++	+	++
Response time	+++	++	+++
Response amplitude	+	+++	+++
Linearity of the response for low concentration	+++	++	++
Reversibility	+++	++	++
Behavior after several exposures	+++	+	++
Global performances	+++	+	++

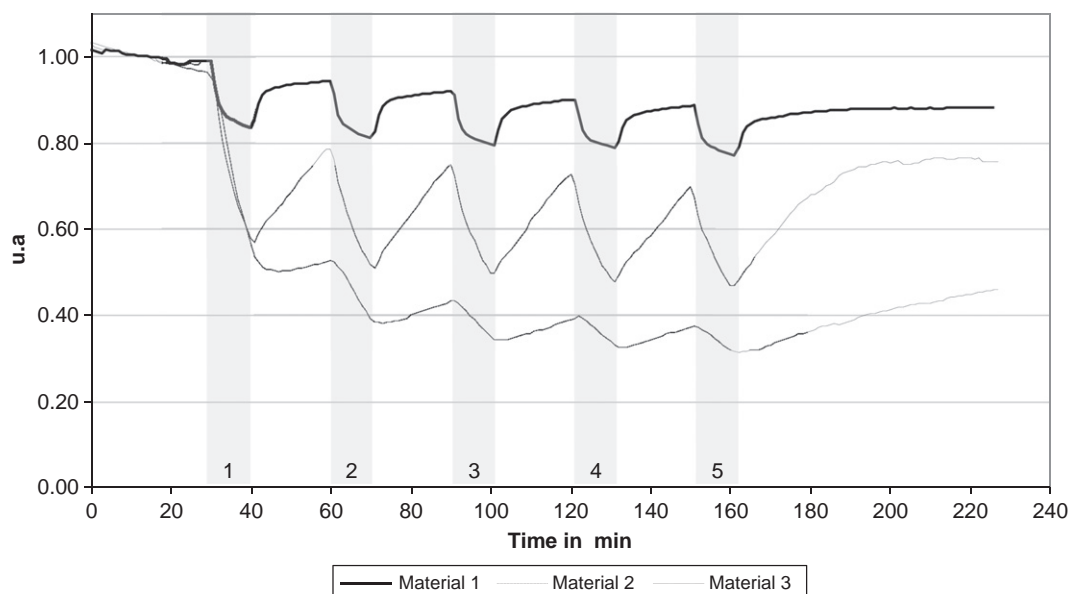


Fig. 5. Fluorescence intensity when the sensors were exposed several times (25 ppb_v of DNT for 10 min following 20 min under dry air).

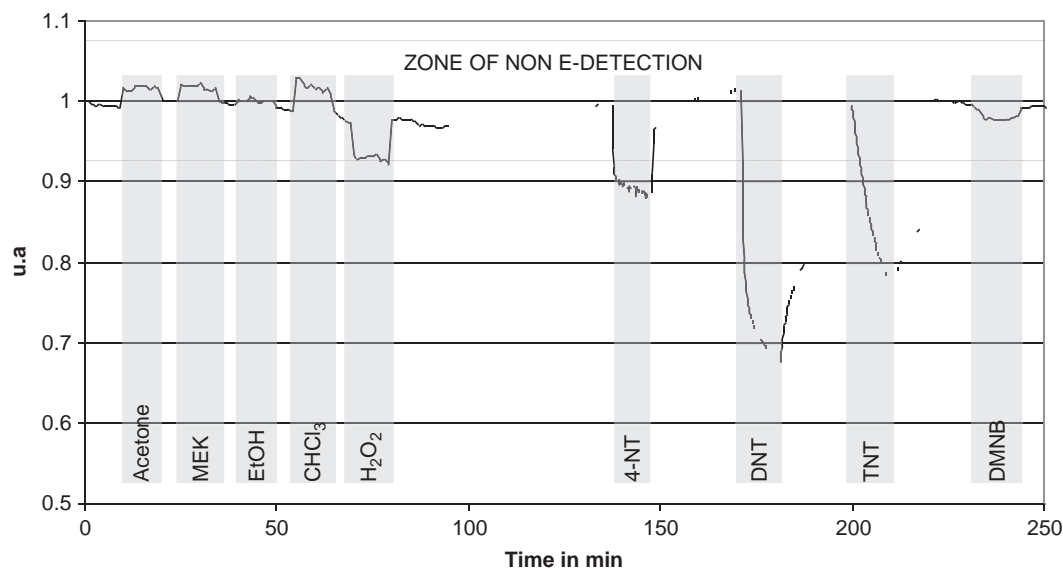


Fig. 6. Fluorescence when the sensor was exposed for 10 min to any analyte and interfering compounds at concentration close to P_{vap} (see Table 2).

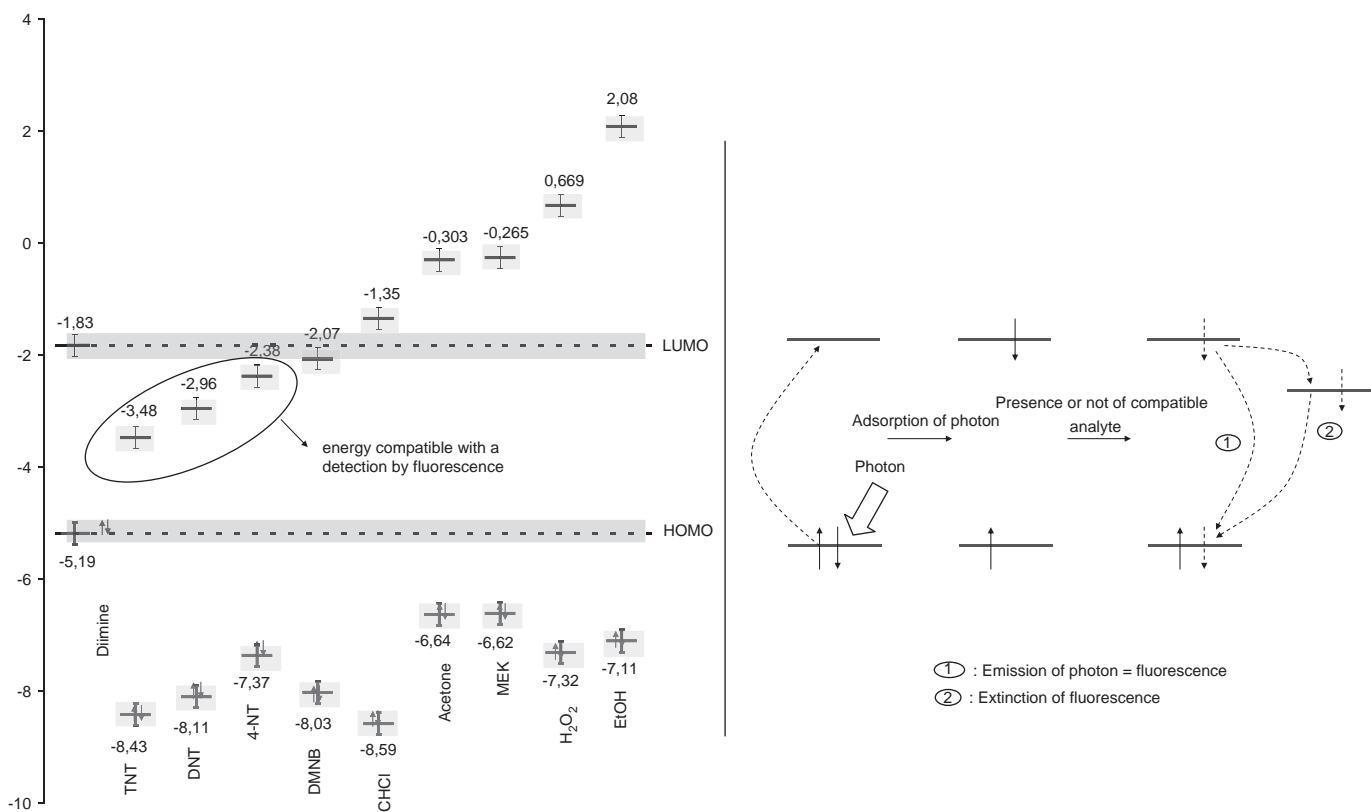


Fig. 7. HOMO and LUMO energies calculated for the various analytes and material 1 at the B3LYP/6-31G* and fluorescence and the charge transfer principle.

compounds, under ambient air, and the responses of the detector are given in Fig. 6. It is interesting to note that only nitroaromatic compounds induced enough fluorescence variation to be detected. In the case of high vapor pressure compounds (acetone, MEK, CHCl_3 , EtOH, and H_2O_2 ; see Table 2), the slight variations of fluorescence were due to optical interference because of the variation of pressure in the detection cell [4]. In the case of the less volatile compound DMNB, the response is close to the response we observed for nitroaromatic compounds but not so large as to be significant.

The inhibition of fluorescence induced by nitro compounds certainly came from a photoinduced charge transfer (PICT) [27]. Theoretical calculations at the B3LYP/6-31G* level of theory were used to determine the HOMO and LUMO energies for the optimized structures of analytes and material 1 [28]. Fig. 7 shows the excited-scale energies of material 1 plotted on the same scale as the molecular orbital calculations for the analytes. The uncertainty of calculation is displayed by a gray zone. Only TNT, DNT and 4-NT were theoretically expected to quench the fluorescence of material 1, as observed by experimental tests.

5. Conclusions

One of the objectives of our research group is to develop a fluorescence detection prototype [1] which detects vapors from nitroaromatic compounds. In this context, the present study concerning the choice of the best sensitive material was realized. The three materials selected for their various structures presented good responses towards DNT. Still, only the conjugated molecule 1 exhibited an excellent reversibility, which conferred an important advantage to this material, rendering possible its use without servicing or calibration between two exposures. Moreover, the performances of this chemical were in line with our objectives in terms of fluorescence intensity, response time, sensitivity and selectivity. It was also shown to be an efficient sensitive material for the detection of TNT despite its low vapor pressure. For these reasons, material 1, a π -conjugated phenylene-ethynylene diimine, was preferred for the development of our prototype.

Acknowledgment

The authors wish to thank Dr. Didier Mathieu for his collaboration in the theoretical calculating at the B3LYP/6-31G**. We also gratefully acknowledge Françoise Serein-Spirau and Jean-Pierre Lère-Porte for their help in the developing of material 1.

References

- [1] T. Caron, S. Clavaguera, M. Huron, P. Montméat, E. Pasquinet, J.P. Lère-Porte, F. Serein-spirau, F. Perraut, P. Prené, *Chem. Eng. Trans.* 23 (2010) 25–30.
- [2] P.A. Pella, *J. Chem., Thermodynamics* 9 (1977) 301–305.
- [3] A. Bardet, F. Parret, M. Guillemot, P. Montméat, P. Prené, *Proceedings of the ISOEN, Brescia*, 2009.
- [4] T. Caron, M. Guillemot, P. Montméat, F. Veignal, F. Perraut, P. Prené, F. Serein-spirau, *Talanta* 81 (2010) 543–548.
- [5] S. Clavaguera, O. Dautel, L. Hairault, C. Méthivier, P. Montméat, E. Pasquinet, C.M. Pradier, F. Serein-spirau, S. Wakim, F. Veignal, J. Moreau, J.P. Lère-Porte, *J. Polym. Sci. Part A: Polym. Chem.* 47 (2009) 4141–4149.
- [6] R.S. Dudhe, J. Sinha, A. Kumar, V.R. Rao, *Sensor. Actuator. B: Chem.* 148 (2010) 158–165.
- [7] S. Kurosawa, N. Kamon, *Langmuir* 8 (1992) 254–256.
- [8] P. Montméat, S. Madonia, E. Pasquinet, L. Hairault, C. Gros, J.M. Barbe, R. Guillard, *IEEE Sensor. J.* 5 (2005) 1–5.
- [9] P. Nelli, E. Dalcanale, G. Faglia, G. Sberveglieri, P. Soncini, *Sensor. Actuator. B: Chem.* 13 (1993) 302–304.
- [10] A.T. Nimal, U. Mittal, M. Singh, M. Khanuja, G.K. Kannan, J.C. Kapoor, V. Dubey, P.K. Gutch, G. Lal, K.D. Vyas, D.C. Gupta, *Sensor. Actuator. B: Chem.* 135 (2009) 399–440.
- [11] F. Parret, P. Montméat, F. Théry-Merland, A. Régien, P. Prené, *Proceedings of the IEEE Sensors, Atlanta, USA* (2007).
- [12] E. Pasquinet, P. Montméat, L. Hairault, R. Amedee, F. Guida, B. Boutevin, F. Ganachaud, *Polycarbosilanes utiles comme matériaux sensibles pour la détection ou le dosage de composés nitrés et capteurs chimiques les comprenant*, Patent FR2929283, 2009.
- [13] J.A.O. Sanchez-Pedreno, P.R.P. Drew, J.F. Alder, *Anal. Chim. Acta* 182 (1986) 285–291.
- [14] M. Schlupp, T. Weil, A.J. Berresheim, U.M. Wiesler, J. Bargon, K. Mullen, *Angew. Chem. Int.* 40 (2001) 4011–4015.
- [15] H. Sohn, R.M. Calhoun, M.J. Sailor, W.C. Trogler, *Angew. Chem. Int.* 40 (2001) 2104–2105.
- [16] B. Xu, X. Wu, H. Li, H. Tong, L. Wang, *Macromolecules* 44 (2011) 5089–5092.
- [17] J.S. Yang, T.M. Swager, *J. Am. Chem. Soc.* 120 (1998) 11864–11873.
- [18] S. Thomas, D.G. Joly, T.M. Swager, *Chem. Rev.* 107 (2007) 1339–1386.
- [19] J.S. Yang, T.M. Swager, *J. Am. Chem. Soc.* 120 (1998) 5321–5322.
- [20] R.A. McGill, M.H. Abraham, J.W. Grate, *CHEMTECH* (1994) 27–37.
- [21] S. Clavaguera, P. Montméat, F. Parret, E. Pasquinet, J.P. Lère-Porte, L. Hairault, *Talanta* 82 (2010) 1397–1402.
- [22] G. Sauerbrey, *Z. Phys.* 155 (1959) 206–222.
- [23] M. Guillemot, F. Dayber, P. Montméat, C. Barthet, P. Prené, *Proceedings of the Eurosensors, Lausanne, Suisse, Poster* 39, 2009.
- [24] J. Rouquerol, F. Rouquerol, K. Sing, *Adsorption by Powders and Porous Solids: Principles, Methodology and Applications* 1998.
- [25] R. Lalauze, *Physico-chimie des interfaces solide-gaz vol.1: concepts et méthodologie pour les l'étude des interactions solide-gaz*, 2006.
- [26] F. Parret, A. Régien, H. Delveaux, F. Veignal, F. Thery-Merland, L. Hairault, P. Montméat, P. Prené, *Récents Progr. Génie Proc.* 96 (2007).
- [27] A. Kumar, M.K. Pandey, R. Anandakathir, R. Mosurkal, V.S. Parmar, A.C. Watterson, J. Kumar, *Sensor. Actuator. B: Chem.* 147 (2010) 105–110.
- [28] J.C. Sanchez, A.G. DiPasquale, A.L. Rheingold, W.C. Trogler, *Chem. Mater.* 19 (2007) 6459–6470.